RADIONUCLIDE INDICATORS OF SEDIMENT DYNAMICS IN THE DELAWARE ESTUARY

by

Joshua L. Humberston

A thesis submitted to the Faculty of the University of Delaware in partial fulfillment of the requirements for the degree of Bachelor of Geological Sciences with Distinction

Spring 2012

© 2012 Humberston
All Rights Reserved

RADIONUCLIDE INDICATORS

OF SEDIMENT DYNAMICS IN

THE DELAWARE ESTUARY

by

Joshua L. Humberston

Approved: ____
Christopher K. Sommerfield, Ph.D
Professor in charge of thesis on behalf of the Advisory Committee

Approved: ____
James E. Pizzuto, Ph.D.
Committee member from the Department of Department Name

Approved: ____
David R. Legates, Ph.D.
Committee member from the Board of Senior Thesis Readers

Approved: ____
Donald Sparks, Ph.D.
Chair of the University Committee on Student and Faculty Honors

ACKNOWLEDGMENTS

Numerous people offered constant support and encouragement over the duration of this senior thesis project. I would like to personally thank Dr. Chris Sommerfield for readily accepting my request to be my thesis director. His support extended beyond the thesis project into my graduate school search and helping me to attend the Ocean Sciences Meeting. I would also like to thank Brandon Boyd, one of Sommerfield’s graduate students, for helping to complete much of the laboratory work for this project. In the field, the crew of the R/V Sharp was helpful, kind, and always made the cruises enjoyable, even in December. I would like to also express my appreciation for Dr. Legates and Dr. Pizzuto who offered up their time to be part of my committee. I would like to thank the NSF for funding my REU which was a gateway into this larger senior thesis project. Finally, I would like to sincerely thank my mom for being available to talk and support me at all times during this year.

TABLE OF CONTENTS

LIST OF FIGURES

ABSTRACT

This report describes the methods and results of a seasonal study of suspended sediment dynamics in the Delaware Estuary using radionuclides as sediment tracers. Specifically, Be-7, I-131, and Pb-210 were used to determine if the estuary at selected coring sites was depositional, and if so, what were the rates of recent deposition. Be-7/Pb-210_{xs} ratios were used to determine relative ages, or time since the sediment was in contact with the water column. Cores from eight sites in the middle to lower estuary were collected in summer, fall, and winter of 2011. Deposition rates varied among coring sites and over time. The absence of Be-7 and I-131 in bed deposits suggest that the estuary at the sampling locations is experiencing no net accumulation. An analysis of deposition variations among cores between seasons suggests large freshwater discharges following Hurricane Irene and Tropical Storm Lee moved the usual depositional zone about 50 kilometers seaward to the lower estuary. Iodine-131 was used to determine general transport distances since it is only sourced in the urbanized estuary.

Chapter 1

INTRODUCTION

Estuarys

An estuary is “an inlet of the sea, reaching into a river valley as far as the upper limit of tidal rise” and is continually altered by freshwater and sediment supplies (Fairbridge, 1980). Estuaries form in coastal river valleys which are drowned by rising sea levels. In general, Atlantic coastal plain estuary systems trap nearly all fluvial and marine sediment (Meade, 1969). There are multiple mechanisms acting to trap sediment in an estuary, but the landward flow of salt water is one of the most recognizable and well-studied trapping mechanisms.

Rivers provide a fresh water source on the landward end of an estuary and the ocean provides a salt water source. Because salt water is denser than fresh water, there is a tendency for the fresh water to flow over top of the salt water that is being pushed into the estuary by gravitational forces. To balance the forces, a salt water front forms in many estuaries where a mean (non-tidal) current of saline water flows landward underneath the fresh water which flows seaward. Sediment that enters the estuary from river and marine sources is then unable to exit the estuary mouth because of this landward flow of salt water. The shape, size, and position of the salt water wedge vary greatly among types of estuaries due to differences in fresh water input, tidal currents, and estuary morphology. In a stratified estuary the salt front is very prominent and the landward mean flow weak, whereas in a weakly stratified or well-mixed estuary, salt water mixing with the freshwater occurs over larger areas and the landward bottom current is weaker.

At its furthest landward reach, the velocity of the mean bottom current drops to zero. This point of the estuary is known as the null zone and represents the point in the estuary where there is theoretically no landward or seaward flow. This null zone, however, may only occur at a small vertical interval of the water column. The null zone is particularly important in sediment studies because it can lead to the formation of an estuary turbidity maximum (ETM). Sediment being carried in the water column flows towards the null zone where it then begins to accumulate and settle due to low water velocity. As sediment accumulates in this area, a noticeable ETM forms where suspended sediment concentrations (SSC) frequently reach high levels of many 10s to 100s of mg/L (Biggs, 1988). Over time, suspended sediment settles and is deposited on the estuary floor. Deposited sediment may remain or later be resuspended and transported to tidal flats on the sides of the estuary where it can more permanently deposited.

Estuary Response to Episodic Events

Increased river input and storm surge currents significantly affect coastal plain estuaries. Besides changing the hydrodynamics of estuaries, storm-generated episodic events produce a huge influx of sediment. In his studies of the James and Rappahannock River estuaries, Nichols founds that “an estimated 90 percent of the average annual suspended load is delivered in less than 11 percent of the time” (Nichols, 1993). Therefore, to understand estuary sediment dynamics, it is crucial to understand depositional patterns resulting from storm events (Nichols, 1993).

Nichols (1993) described a coastal plain estuary's response to a storm event in a four step sequence which includes an initial response phase, a shock phase, a rebound phase, and a recovery phase. The entire sequence lasts from about seven to 22 days or more. During the initial response as a storm approaches, the net landward flow increases for a short period and then drops back to normal levels. Near-bottom suspended sediment concentrations tend to increase by at least 5 fold as storm surge currents and wave resuspension increase. As the storm hits the estuary and its watershed, the shock phase begins. The shock phase is characterized by high rainfall and river flooding. The increased input of freshwater from rivers pushes the net current in the upper estuary seaward, resuspending bed sediment and transporting it seaward. In the lower estuary, Nichols found that a partially mixed estuary became highly stratified. In his studies, the estuarine turbidity maximum was destroyed at its known site but eventually reformed at a further seaward location. Three to six days after the storm, river flows begin to return to normal as does sediment influx to the estuary. A strong landward flow with high sediment concentrations forms as the turbidity maximum shifts landward again. The final phase, recovery, begins after about seven days and can be recognized by relatively normal flow velocities, sediment levels, and less stratification. During the recovery phase, the turbidity maximum returns to its normal area and is generally less intense. Nichols also found that sediment derived from the storm event is stored landward of the freshwater-salt water convergence or farther seaward in the closed estuarine circulation (Nichols, 1993).

The Delaware Estuary

The Delaware Estuary is an urbanized coastal plain estuary stretching 215 km from the mouth of the Delaware Bay to the head of tides at Trenton, NJ (Lebo et al., 1993; Cook et al., 2007).The estuary and bay form the second largest estuary system on the U.S. Atlantic East Coast and are second in ship traffic only to the New York Harbor (Cook, 2002). In order to maintain an adequate depth in the main shipping channel, the upper estuary is regularly dredged and the sediment is permanently removed. The Delaware Bay also serves an important role ecologically; its shores host the largest population of spawning horseshoe crabs in the world. Horseshoe eggs which are deposited along the shores of the bay area crucial food source for migrating shore birds (Howel, 2011). The amount of sediment imported to the estuary, its residence time, and its composition are crucial to the estuary's morphology and ecological health (Nichols and Biggs, 1985). For the estuary's ecology, muddy sediment is a source of important nutrients like phosphorous and organic carbon. Sediment filled marshes surrounding much of the Estuary provide a filtering system for harmful contaminants from local farms and other waste sources. Sediment dynamics, therefore, play a large role in the estuary's ecosystem.

Each year, about 1.3×10^9 kg of suspended river sediment is delivered to the Delaware Estuary from fluvial sources (Mansue and Commings, 1971; Walsh, 2004). In conjunction with the Delaware Bay, the estuary system captures essentially all incoming fluvial and marine sediment (Sommerfield and Wong, 2011). Due to a large tidal discharge relative to the fresh water input, the estuary is considered a weakly stratified system. An ETM with surface suspended-sediment concentrations (SSC) on the order of 10-100 mgL^{-1} typically exists 50-120 km from the bay mouth as a result of residual gravitational flow (Biggs et al., 1983; Sommerfield and Wong, 2011).

While there have been numerous studies exploring large scale hydrodynamics in the Delaware Estuary (Pape and Garvine, 1982; Wong and Garvine, 1984; Janzen and Wong, 2002) details regarding the behavior of sediment are still sparse. Recent research has shed much light on sediment dynamics in the Delaware Estuary (Cook et al., 2007; Sommerfield and Wong, 2011), but there remain gaps in knowledge. The large size and complicated circulation of the estuary give rise to highly variable suspended sediment concentrations and bottom sediment characteristics, which makes it difficult to predict sediment-transport pathways and rates of movement. From sediment-flux measurements it has been found that residual gravitational circulation, tidal velocity asymmetry, and tidal mixing asymmetry influence sediment transport and turbidity levels in the estuary (Sommerfield and Wong, 2011). However, sediment source areas, residence times, and centers of deposition cannot be determined from flux measurements alone. Other methods are needed to address how suspended sediment moves into and around the Delaware estuary.

Radionuclides as Sediment Tracers

For years, naturally occurring radionuclides have been used to trace sediment and measure deposition in support of environmental studies (e.g., Olsen et al., 1986). Beryllium-7 ($t_{1/2}$=53.3 days) and Pb-210 ($t_{1/2}$=22.3 years) are two well-known indicators of estuary sediment dynamics (Matisoff et al., 2005). Beryllium-7 and Pb-210 are delivered to aquatic waters from the atmosphere mostly in precipitation. In the water column, the radionuclides associate with sediment particles through cation exchange (Fitzgerald et al., 2001). In bed sediment, Be-7 can be used to indicate short term sediment deposition because of its short half-life. Since Pb-210 and Be-7 both have a cosmogenic source, Matisoff et al. (2005) found that Be-7/ Pb-210 ratios can be used to predict relative ages of sediment. Be-7 activities decrease noticeably during a few weeks, but Pb-210 decay is negligible because of its longer half-life. Therefore, the Be-7/ Pb-210 ratio decrease with depth and constrains the time since the sediment was labeled with the radionuclides.

More recently, Smith et al. (2008) described another radionuclide, I-131 ($t_{1/2}$=8 days), as “a potential short-lived, wastewater-specific particle tracer in an urbanized estuarine system” (Smith et al, 2008). Iodine-131 is a fission-produced radioisotope which “is used as a radiopharmaceutical for medical imaging, diagnostics, and treatments for conditions of the thyroid” (Smith *et al*. 2008). Following its medical use, it is introduced to the waste stream at both hospitals and released patient’s homes where it is then transported to waste-water release sites along some urbanized estuaries. The work of Smith et al. (2008) was limited to the lower Hudson River Estuary, but these authors suggested that I-131 has potential use as a sediment tracer in other urban estuaries. Measurements of Delaware Estuary water and bed sediments by Dr. Sommerfield in 2010 and 2011 revealed the presence of I-131 in both suspended and bottom sediment (Sommerfield and Duval, 2012). Sommerfield has found that I-131 is being introduced to the Delaware Estuary as multiple waste water treatment plants along the upper, highly urbanized segment of estuary. I-131 has been detected in suspended sediment throughout the Delaware Estuary and in the lower Delaware River landward of the head of tide (Trenton, New Jersey). However, I-131 is not being released into the water seaward of Wilmington, so its presence down-estuary provides a source-specific tracer of water and particles from upper estuary sources.

Chapter 2

METHODS

Field

Samples for this project were collected during cruises of the R/V *Sharp* in summer, fall, and winter 2011. Freshwater discharge to the estuary during the study period is shown in Figure 1. Seabed cores were collected at nine sites, labeled ‘A’ through ‘I’, along the middle to lower Delaware Estuary using a short gravity corer. The weighted corer was dropped down off the side of the vessel and retrieved using a vessel-mounted crane. Care was taken to preserve an intact sediment-water interface for the cores, which were generally 20-24 cm in length and composed of soft mud. After recovering a core, it was taken into an onboard wet lab intact. In the wet lab, cores were dissected into 2 cm thick sections beginning at the sediment-water interface. Each section was placed in a plastic bag to be stored for the remainder of the cruise. During each cruise, a CTD sled was deployed to profile water column salinity and turbidity at 23 sites from the mouth of the bay to the head of tide. Upon return to shore, the bags of bottom sediment were immediately transferred to a refrigerator for storage.

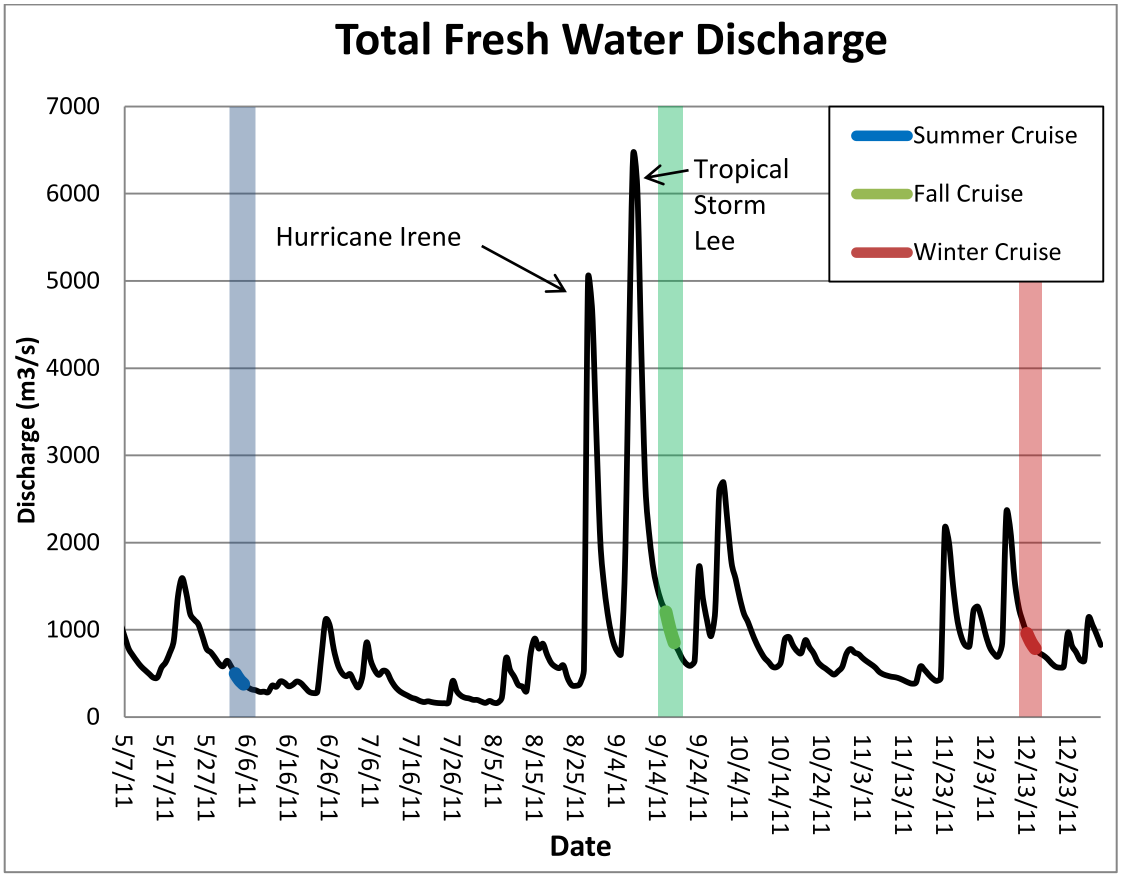

Figure 1 Freshwater discharge of the Delaware River at Trenton during the study period.

Lab

Beginning with the surface sections, which were most likely to contain short-lived radionuclides, the wet sediment samples were placed in weighed jars and then reweighed. After obtaining the wet mass of the sediment, the samples were placed in an oven at 100˚C to dry for one to two days. Once dry, the samples and their jars were reweighed to determine the initial water content. This was used to determine porosity and dry-bulk density. Next, using a mortar and pestle, the samples were ground into a fine powder and put into weighed plastic containers. The powdered samples were pressed firmly into the containers to maintain a consistent sample size. The samples were then reweighed and a lid was placed on each. The samples were then thoroughly brushed clean and taken to a separate room for gamma spectrum analysis. The samples were analyzed within two weeks of sampling to capture short-lived I-131 and Be-7, and recounted several months later (by Dr. Sommerfield's group). The second round of counts was conducted to determine if Pb-210 was in secular equilibrium with its parent nuclides (Rn-222→Ra-226) at the time of initial counting. Gaseous Rn-222 can be lost during sample preparation and from the sample container thus reducing measured activity of Pb-210. The second counting confirmed secular equilibrium and accuracy of the initial Pb-210 counts.

Next, each sample was individually placed in a Canberra low energy germanium detector (LEGe). Liquid nitrogen, which is used to supercool the detector, was added to the dewars before or after counts to avoid any interruption. Each sample was counted for a 24-hour time period to allow for sufficient gamma counts from the naturally occurring radionuclides. A computer connected to each detector recorded the counts detected at each energy level from 25 to 700 keV.

Data Analysis

On the resulting gamma count spectrum, photopeaks were picked out and marked as regions of interest (ROI) for seven radionuclides: Pb-210, Th-234, Pb-214, I-131, Be-7, Bi-214, and Cs-137. Using the Canberra analyzing software, gamma peaks were integrated to find the area under the radionuclide photopeak minus the continuum background counts. If the number of counts for a photopeak was below a set critical limit, the peak was not considered significant. Following methods described by Wallbrink et al. (2002), the specific activity (activity/dry mass) of the radionuclide was computed taking into account the background activity and the efficiency of the gamma detector (Equation I).

Equation I

$$\text{Specific activity (Bq/kg)} = A = \left(\frac{C}{T} - \frac{C_b}{T_b}\right) \cdot \frac{1}{M \cdot \varepsilon_A}$$

Where:

c = *total counts (above continuum background)*
T = *sample count time (s) [1 day = 86400 s]*
$\frac{C_b}{T_b}$ = *efficiency correction*
M = *Sample mass*
ε_A = *Activity Efficiency*

Corrections were made to the specific activities to account for the decay which took place between collection and counting. Corrections were also made to determine excess Pb-210 activity (from atmospheric fallout of Pb-210 and particle adsorption) from the total measured activity. For this technique, supported Pb-210 activity (by decay of mineral-bound Ra-226) was subtracted from the total Pb-210 to obtain excess activity.

Activity-depth plots were constructed for cores which exhibited radionuclides of interest below the surface section and the shape of the profiles was used to compute the deposition rates. The differences in deposition rates and inventory among the coring sites were used to investigate sediment sedimentation rates and in the case of I-131, transport pathways and transit times. Relative ages were determined using the methods and equations described by Matisoff et al. (2005) (Equation II).

Equation II

$$t = -\frac{1}{\lambda_{Be7} - \lambda_{Pb210}} \ln\left(\frac{A}{B}\right) + 14$$

Where:

t = Relative age (days)
λ_{Be7} = 0.01300 d^{-1}
λ_{Pb210} = 8.50999 × 10^{-5} d^{-1}
A = decay corrected Be-7 activity
B = decay corrected $Pb\text{-}210_{xs}$ activity

In this equation, it is assumed the Be-7 and Pb-210 are introduced into the system at the same ratio throughout time. Equation II accounts for the change in that ratio and is therefore relative to that initial ratio.

Beryllium-7 inventories were calculated for cores from sites A, F, and I. Inventories represent the total, depth-integrated radionuclide activity in the sediment column. Using the residual inventory method described by Canuel et al. (1990), expected inventories were calculated for sites A, F, and I by decay correcting the prior season's radionuclide activities. A measured inventory higher than the calculated inventory suggests additional deposition and a lower measured inventory suggests loss of inventory, possibly by erosion between the time of initial and subsequent sampling.

Equation III

$$I_2 = I_1 \times e^{-\lambda t}$$

Where:

I_2 = Inventory at time after time (t)
I_1 = Initial Inventory
λ = Decay Constant
t = time (days)

Chapter 3

RESULTS

Introduction

Of the 9 sites cores were collected at each season, sites A, F, and I showed the most valuable radionuclide data. The locations of these sites are shown in Figure 2. The other coring sites showed little to no Be-7 and I-131 activity, suggesting that deposition does not normally occur around those locations. While knowing areas of non-deposition is valuable to understanding sediment dynamics in the estuary, cores with continuous activity or varying activity are more useful in determining seasonal changes in depositional patterns. Therefore, the results presented are primarily from sites A, F, and I where activity levels were above the critical limit and thus considered significant. The absence of data for any particular core does not mean that data was not collected, but only that it did not meet the criteria to be considered significant. Beryllium-7 inventories were determined for cores and are expressed in terms of total activity per square centimeter of surface area.

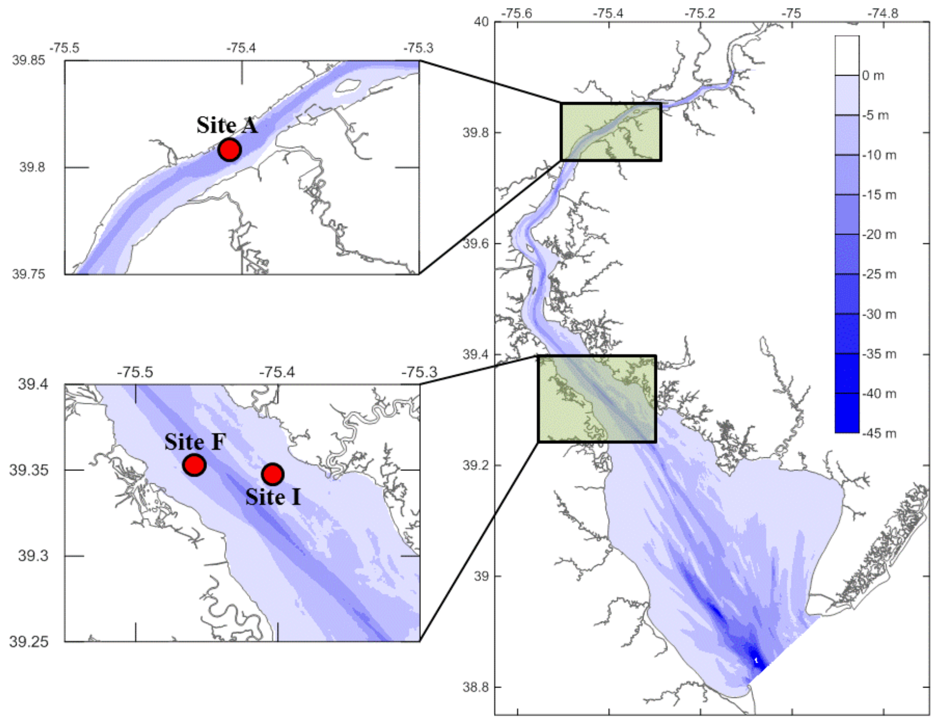

Figure 2 Base map of study area with coring sites A, F, and I marked in zoomed in areas.

Summer

Core data from the summer cores is presented in Appendix A. At site A, Be-7 and I-131 activity decreased down the core. Be-7 activity was measureable to the core bottom, and I-131 was detected to 6 cm (Figure 3-b, 3-c). The total inventory of Be-7 was calculated to be 115 mBq/cm^2. At site F, Be-7 activity was lower than at Site A (Figure 4-b). The total inventory was calculated to be 24mBq/cm^2. No I-131 activity was detected in this core. Near-surface sections (0-2 cm sediment depth) of the core from Site I showed lower activity levels of Be-7 than deeper sections (Figure 5-b). There was a decreasing trend in Be-7 activity beginning at the 6-8 cm section. The total Be-7 inventory from the site I core was actually the highest from the summer cruise at 118 mBq/cm^2. No I-131 activity was detected in Core I. Be-7/xsPb-210 ratios showed a net decreasing trend down at Sites A, F, and I, thus there is a general increase in relative age, or time since Be-7 was introduced to the water column, down the cores (Figures3, 4, 5). Be-7 was detected in notable amounts at Sites A, B, F, and I. I-131 was only detected in significant amount at Site A and B.

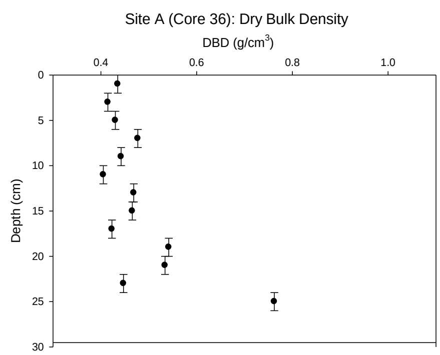

Figure 3-a

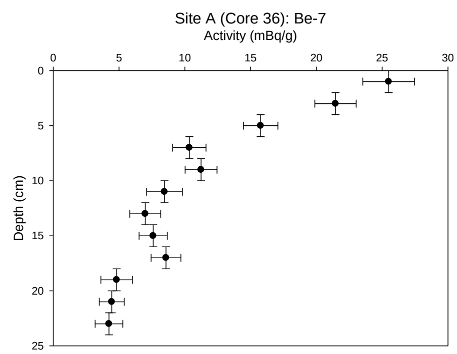

Figure 3-b

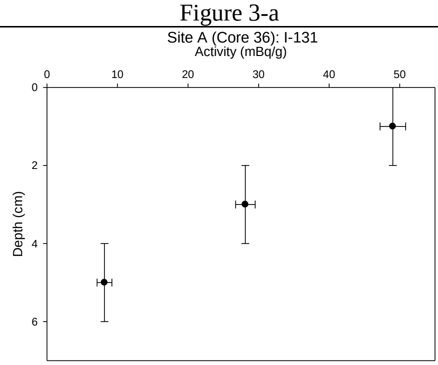

Figure 3-c

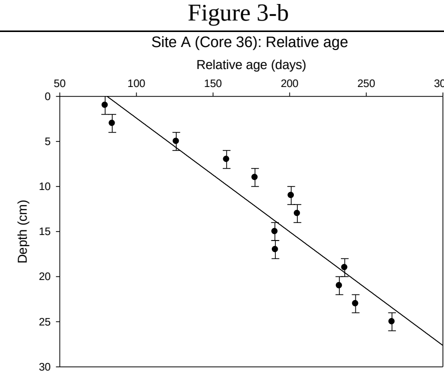

Figure 3-d

Figure 3 Summer: Depth profiles of DBD, radionuclide activities, and relative age from core 36 (site A). Be-7 and I-131 show decreasing activity down core. The relative age of sediment increases down core.

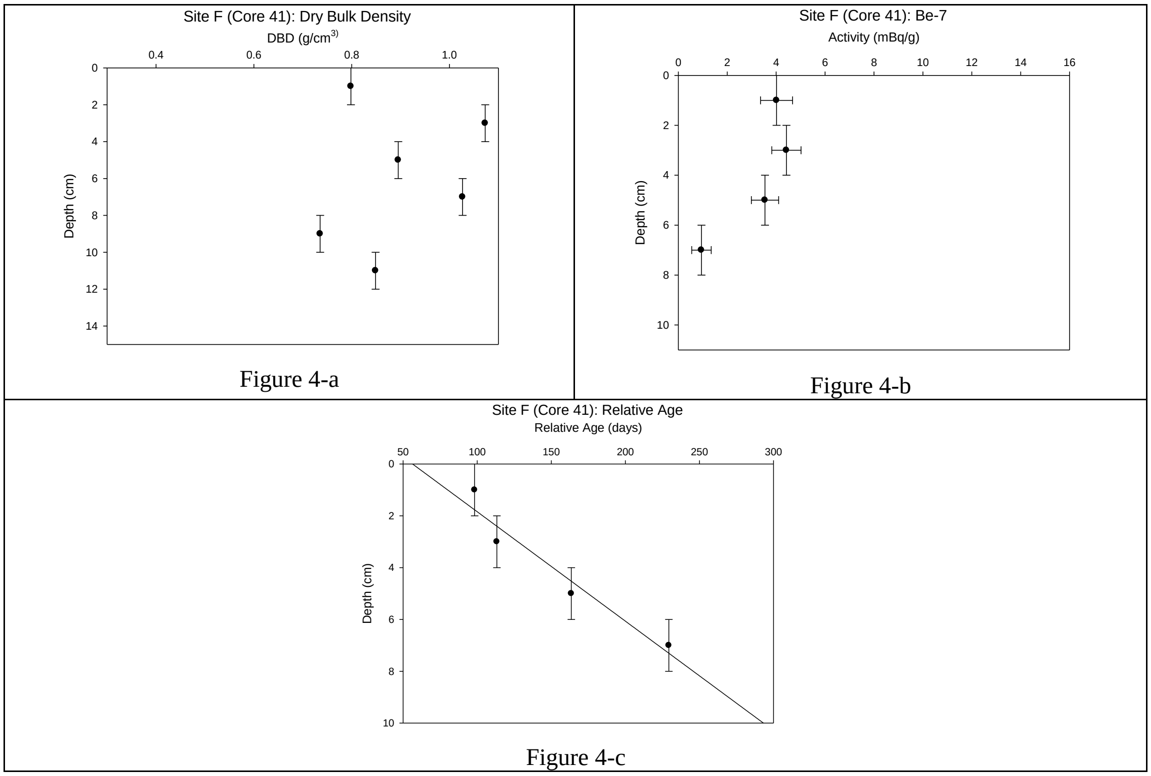

Figure 4 Summer: Depth profiles of DBD, radionuclide activities, and relative age from core 41(Site F). Be-7 activity is lower than in core 36 but still significant and shows a decrease down core.

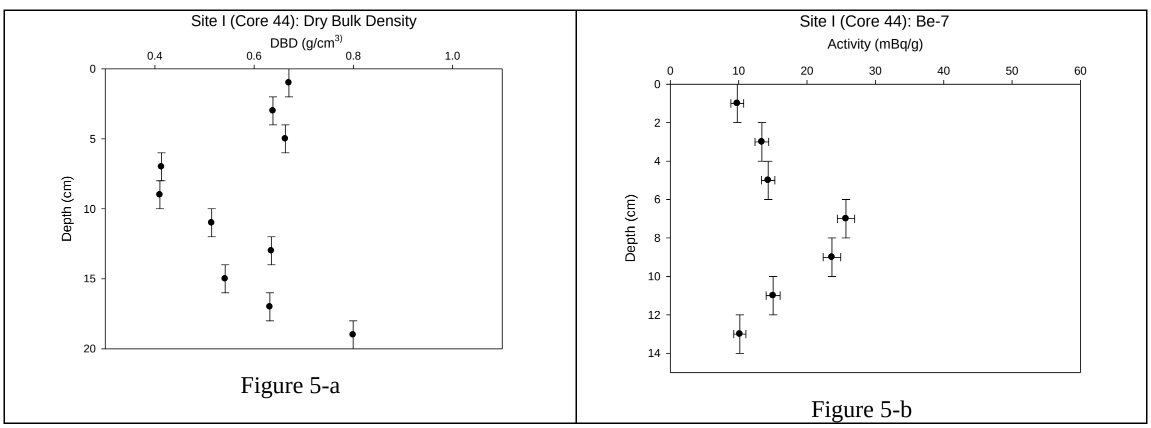

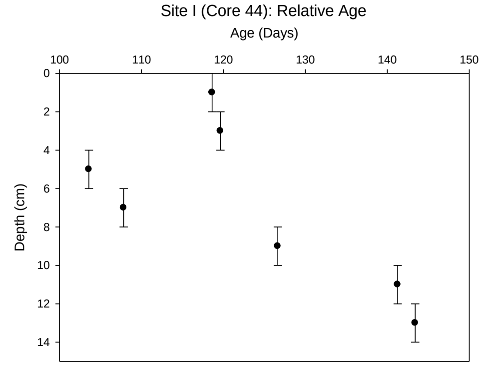

Figure 5-c

Figure 5 Summer: Depth profiles of DBD and radionuclide activities from core 44 (site I). Be-7 and DBD have nonlinear trends in the top 10 cm.

Fall

The data from the fall cores is presented in Appendix B. In the core collected at site A in fall, Be-7 activity above the critical limit was measured down to 22 cm, though activities were lower than in the Summer (Figure 6-b). I-131 was not detected at significant levels at Site A. As expected, the relative ages of the sediment generally increased down core (Figure 6-c). Site F also showed Be-7 activity, but no I-131 activity. Be-7 was only detected above the critical limit levels down to 10 cm depth (Figure 7-b). Site I shows much higher Be-7 than in summer and I-131 was present (Figure 8). Be-7 activity was above critical limits down to 12 cm depth and I-131 activity was above critical limits down to 6 cm depth (Figure 8-b, Figure 8-c). This core site was the only site in the lower estuary where significant I-131 activities were measured at any depth during any season. The relative age of the sediment is very similar within the top 6 cm at Site I and then increases rapidly (Figure 8-d).

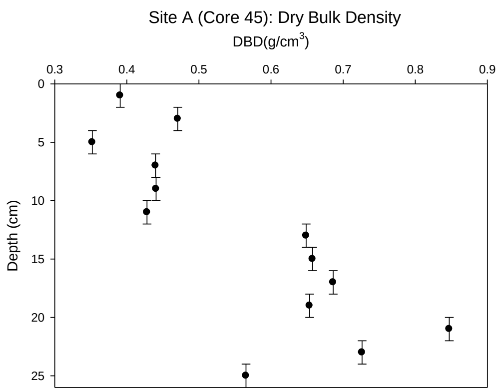

Figure 6-a

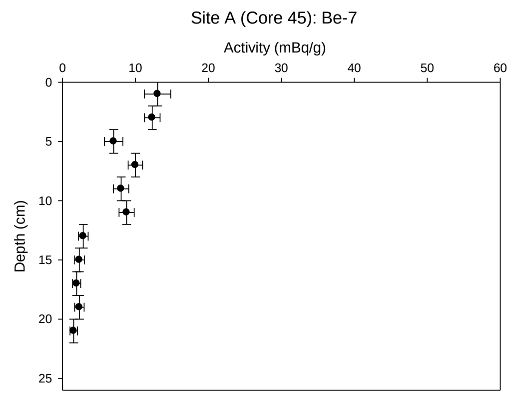

Figure 6-b

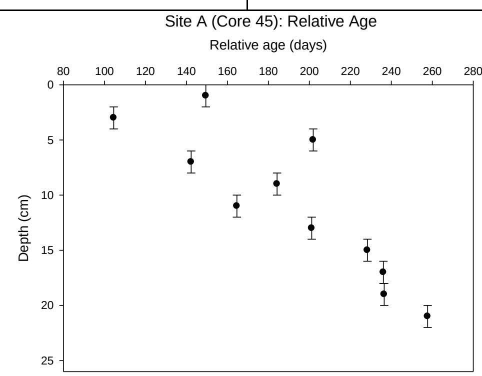

Figure 6-c

Figure 6 Fall: DBD, Be-7, and Relative Age of Core 45 (site A). There is a general decrease in DBD and Be-7 activity measurements with increasing depth. No significant I-131 activity was detected.

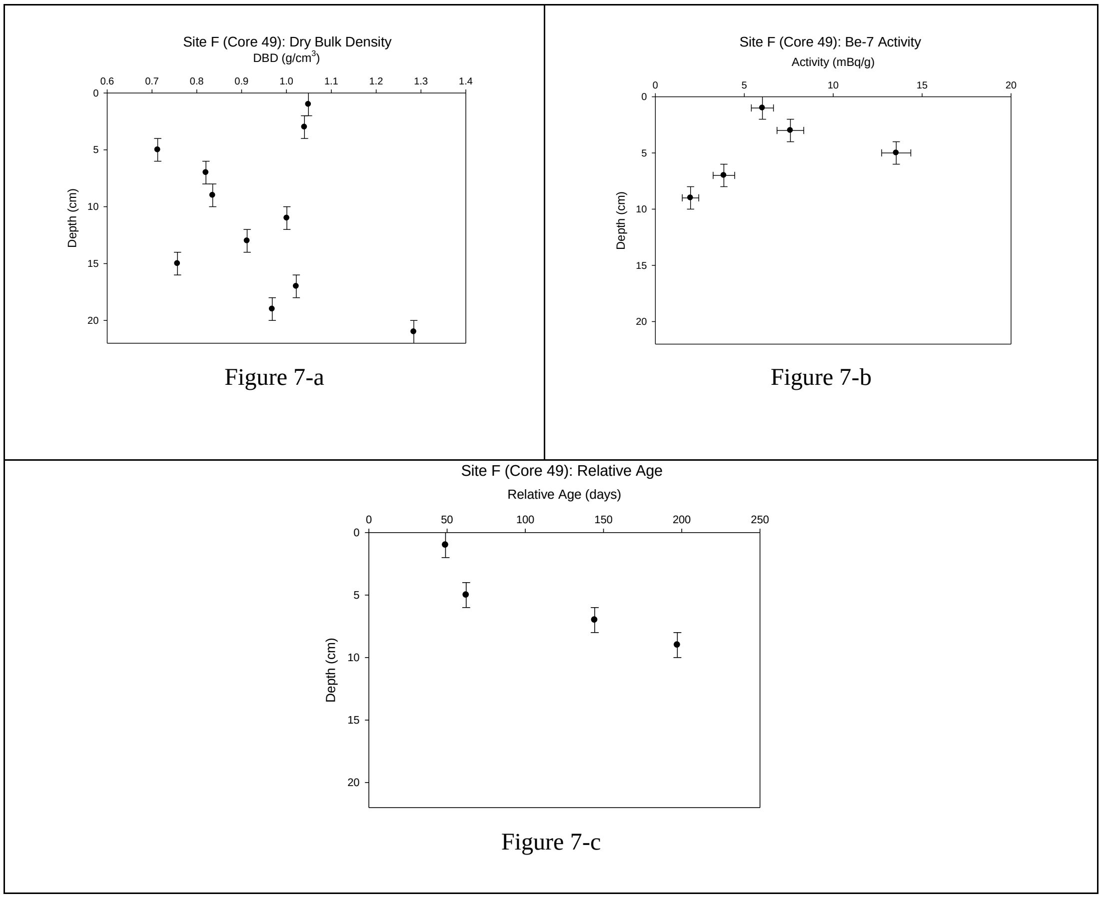

Figure 7 Fall: Depth profiles of DBD, Be-7 activity, and relative age from core 49 (site F). The relative age of sediment increases down core.

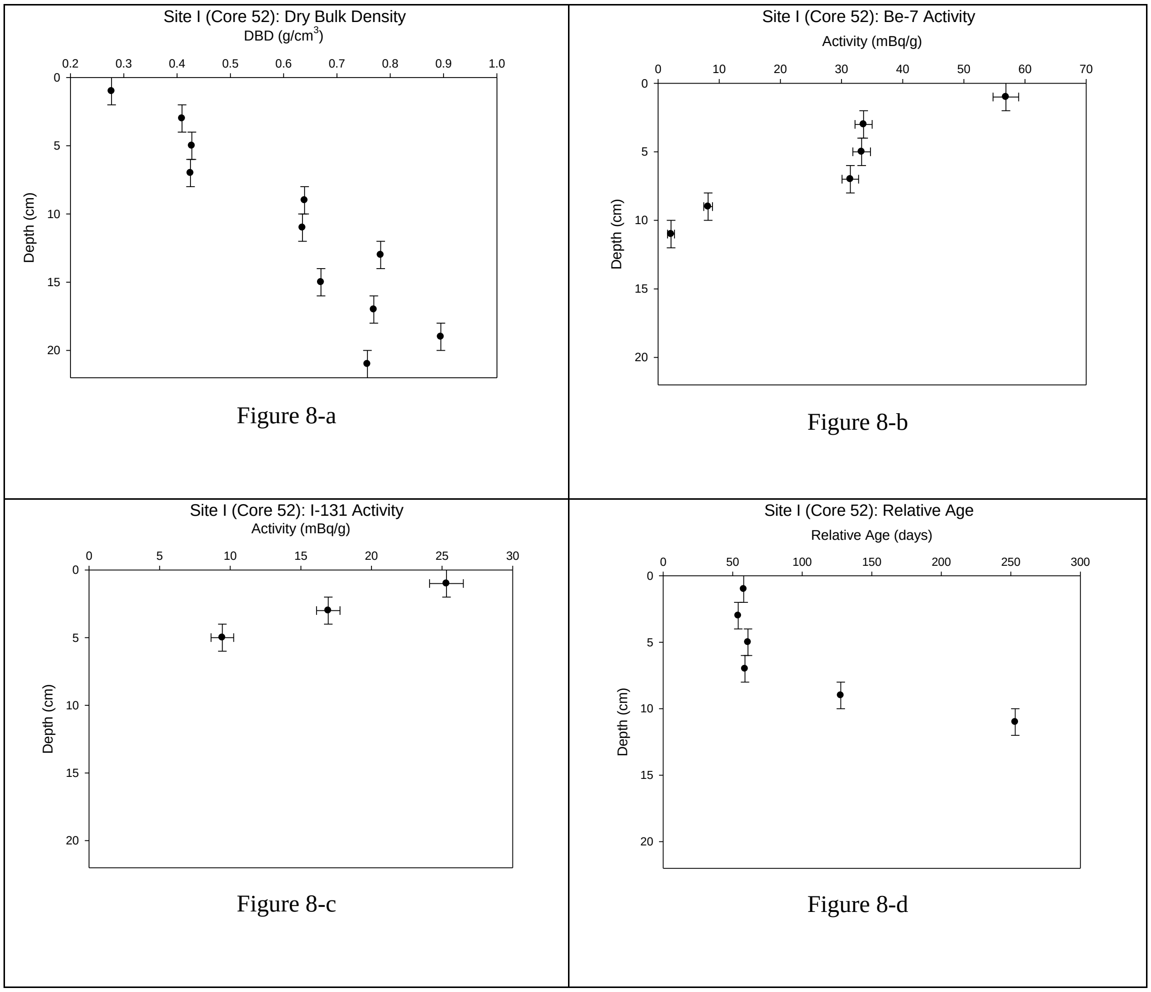

Figure 8-a

Figure 8-b

Figure 8-c

Figure 8-d

Figure 8 Fall: Depth profiles of DBD, Be-7 and I-131 activities, and relative age from core 52 (site I). The relative age of the sediment is similar in the top 8 cm and then decreases more rapidly.

Winter

Core data from the winter cores is presented in Appendix C. Site A again had both Be-7 and I-131 activity in winter (Figure 9). Be-7 was present down to 8 cm depth (Figure 9-b) with an inventory of 29 mBq/cm^2 and I-131 was present down to 6 cm depth (Figure 9-c). At Site F, Be-7 was detected down to a depth of 6 cm with an inventory of 23 mBq/cm^2. No I-131 was detected (Figure 10). Site F never showed any I-131 activity during any season. Site I continued to show Be-7 activity, but I-131 was not detected in winter (Figure 11). Be-7 was detected above the critical limit down to 10 cm depth (Figure 11-b) and had an inventory of 44 mBq/cm^2.

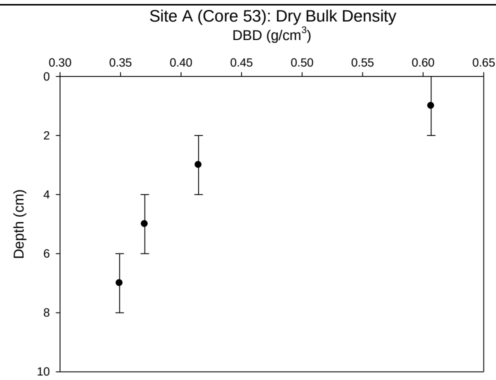

Figure 9-a

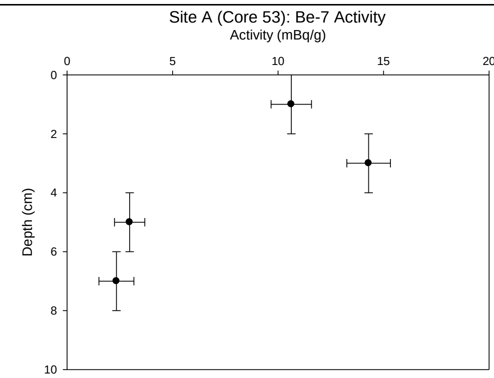

Figure 9-b

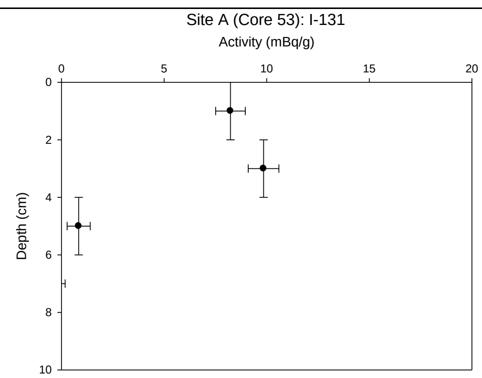

Figure 9-c

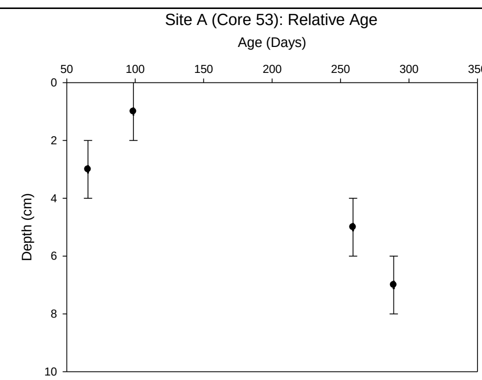

Figure 9-d

Figure 9 Winter: Depth profiles of DBD, radionuclide activities, and relative age from core 53 (site A).

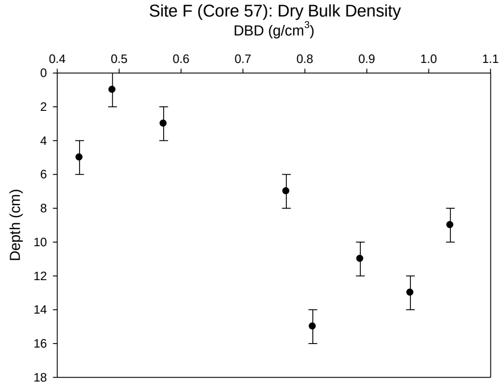

Figure 10-a

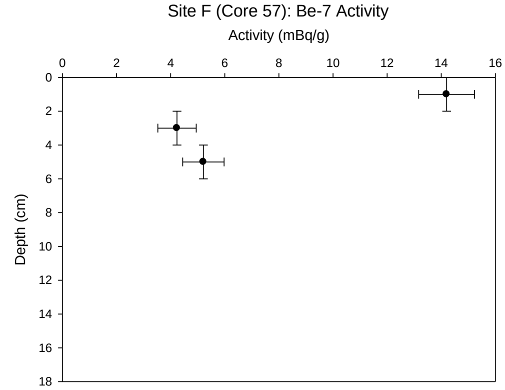

Figure 10-b

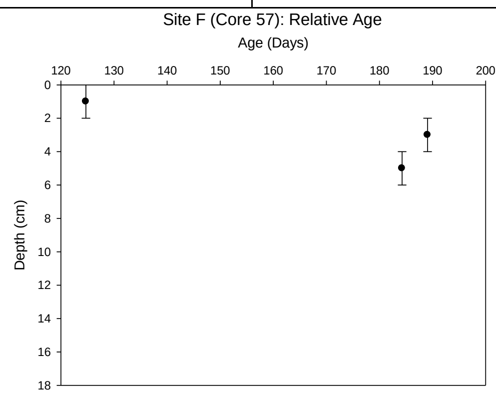

Figure 10-c

Figure 10 Winter: Depth profiles of DBD, Be-7 activity, and relative age from core 57 (site F). Significant levels of Be-7 were only measured down to 6 cm depth.

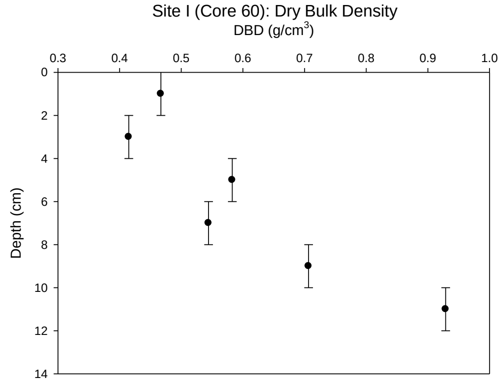

Figure 11-a

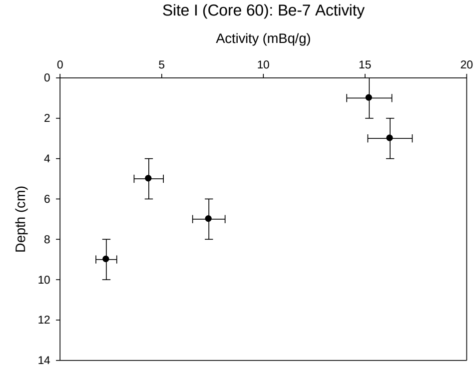

Figure 11-b

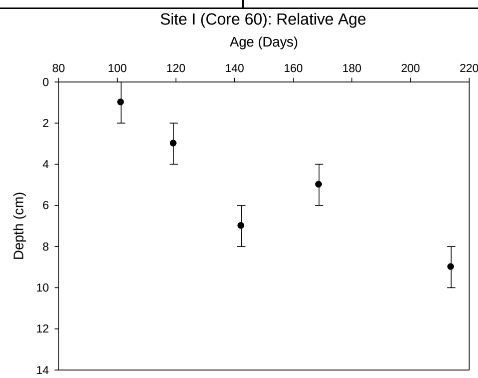

Figure 11-c

Figure 11 Winter: Depth profiles of DBD, Be-7 activity, and relative age from core 60 (site I). The relative age of sediment generally increases with depth. No I-131 was measured at site I in winter.

Chapter 4

DISCUSSION

Introduction

This study looked into not only how sediment deposition changes in the Delaware Estuary on a seasonal basis, but also how deposition is affected by an episodic event such as a hurricane. Cores collected in the fall season were obtained just days after the passing of Tropical Storm Lee, which was closely preceded by Hurricane Irene. Fresh water discharge was notably increased by both storm systems and remained above normal levels during the fall core collection period (Figure 12). The original goal of analyzing variations in normal seasonal deposition was adjusted to account for the atypical events prior to fall core collection.

In general, each season is predicted to represent the Delaware Estuary under different conditions. The summer cruise followed a time of moderate river discharge and the results therefore typify the estuary's circulation and depositional patterns under relatively normal conditions. As a result of Hurricane Irene and tropical storm Lee, the fall samples represent depositional patterns following a large episodic event in the estuary. The winter samples portray the depositional patterns of a recovering estuary. At the time of the winter cruise, the estuary was probably still progressing towards its normal state following a combination of storms during the fall and winter. Freshwater discharge was still quite high during the Winter Cruise.

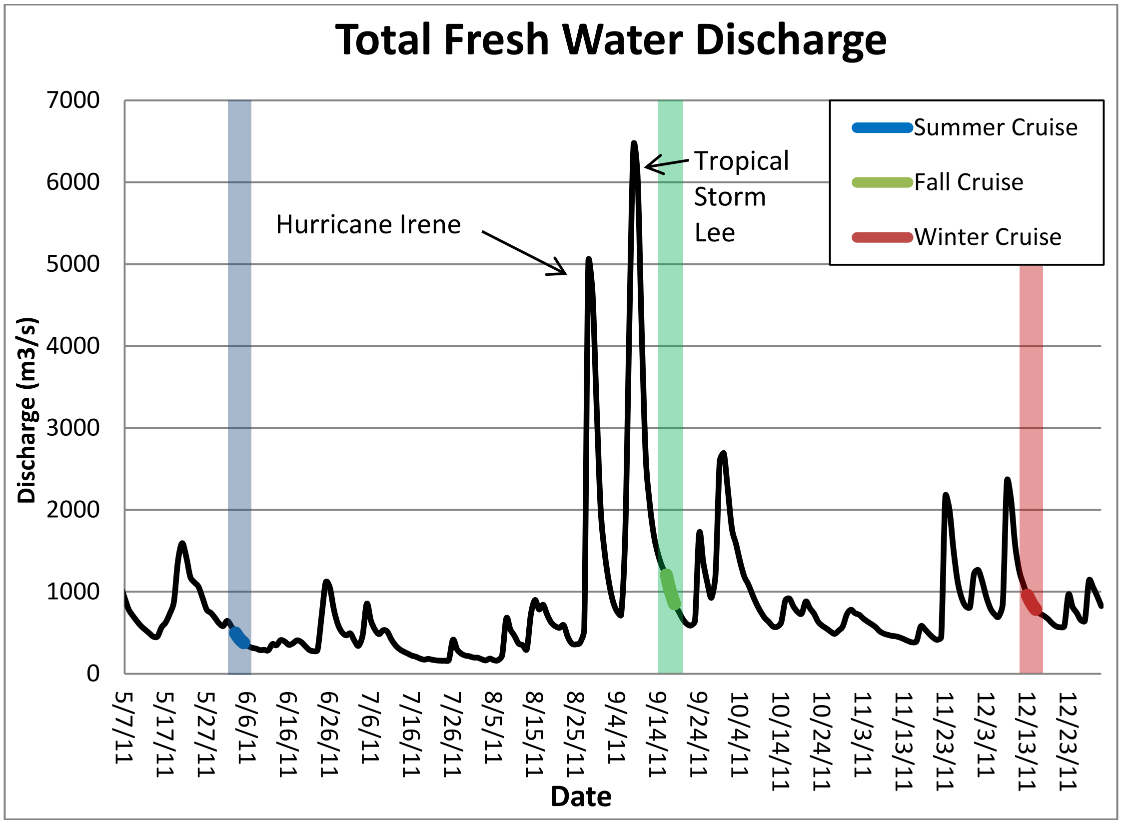

Figure 12 Total Fresh Water Discharge into the Delaware Estuary with cruise dates marked. The total fresh water discharge is the collective discharge of the two primary rivers, the Delaware River and the Schuylkill River)

Summer

Based on previous work done by Summerfield and Wong (2010), it was determined that the summer results best represented the Delaware Estuary during relatively normal conditions. Maximum deposition was measured at sites A which is located about 130 km inland of the bay mouth. Deposition rates were fairly significant and consistent, averaging at about 5 cm per 50 days in the top 25 cm as determined by the relative age (Figure 2-d).However, while site I, located about 70 km landward of the bay mouth, did not show a consistent depositional trend (Figure 4-c), it actually showed the highest Be-7 inventory suggesting high amounts of recent deposition. An estimated 10 cm were deposited within a 50 day time period at site I. Site F, located near site I, also showed significant deposition. The deposition rate at site F was about 1cm per 50 days (Figure 3-c).

Suspended sediment concentrations measured during the cruises revealed the ETM was located about 75 km inland of the bay mouth (Figure 13). High SSC were still present in the area of site A, likely accounting for the high deposition in that area. There were also cores in the vicinity of the observable ETM that did not exhibit deposition. This is believed to be due to bed forms which were seen using a side scanning sonar device during the fall cruise. Due to bottom currents, ripples form along the bottom and cause sediment to rapidly accumulate in some areas and not in others. Sites A, I, and F likely contained bed forms composed of recently deposited sediment on the bottom while some other sites, such as site B, show areas where deposition does not normally occur.

Using the samples with significant deposition to represent general areas of deposition, it is believed maximum sediment deposition occurred in the known area of the ETM, about 75 km landward of the bay mouth, and further landward. It is possible that deposition at site A is fluvial sourced sediment falling out of the water column due to lessening water velocities. Deposition at sites F and I are most likely due to the presence of the ETM and null zone. The null zone, which is characterized by no net seaward or landward flow, allows even fine grained sediment to settle out of the water column.

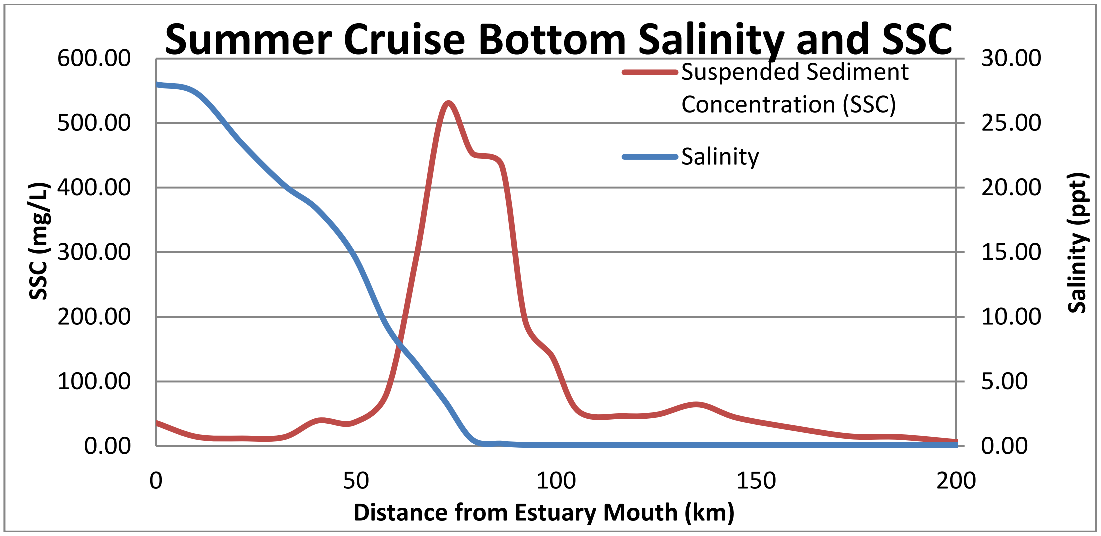

Figure 13 Bottom Suspended Sediment Concentration and Salinity from an axial survey of the estuary during the summer cruise.

Fall

As can be seen in Figure 14, the fall cruise occurred shortly after two periods of extremely high fresh water discharge. Tropical storm Lee, which occurred after Hurricane Irene, actually produced a larger fresh water discharge. The larger discharge is likely due to increased run off caused by already saturated ground in the watershed. Collectively, the two storm events clearly had a dramatic event on the estuary hydrodynamics and sediment dynamics. Figure 14 also shows that suspended sediment concentrations were slightly elevated between 50 and about 175 km landward of the bay mouth, even a week after the peak freshwater discharge. In general though, SSC were actually lower than during the summer cruise, possibly as the result of lowered sediment input from rivers. The extremely large freshwater discharge events may have scoured the rivers leaving less sediment to be transported following the events. Two distinct peaks can be seen in the SSC, one at about 100 km and one at about 140 km (Figure 14). Biggs et al (1983) measured two separate and distinct turbidity maxima in the Delaware Estuary. Further studies by Sommerfield (2011) helped confirm the presence of two turbidity maxima which appear to have been present at the time of the fall cruise.

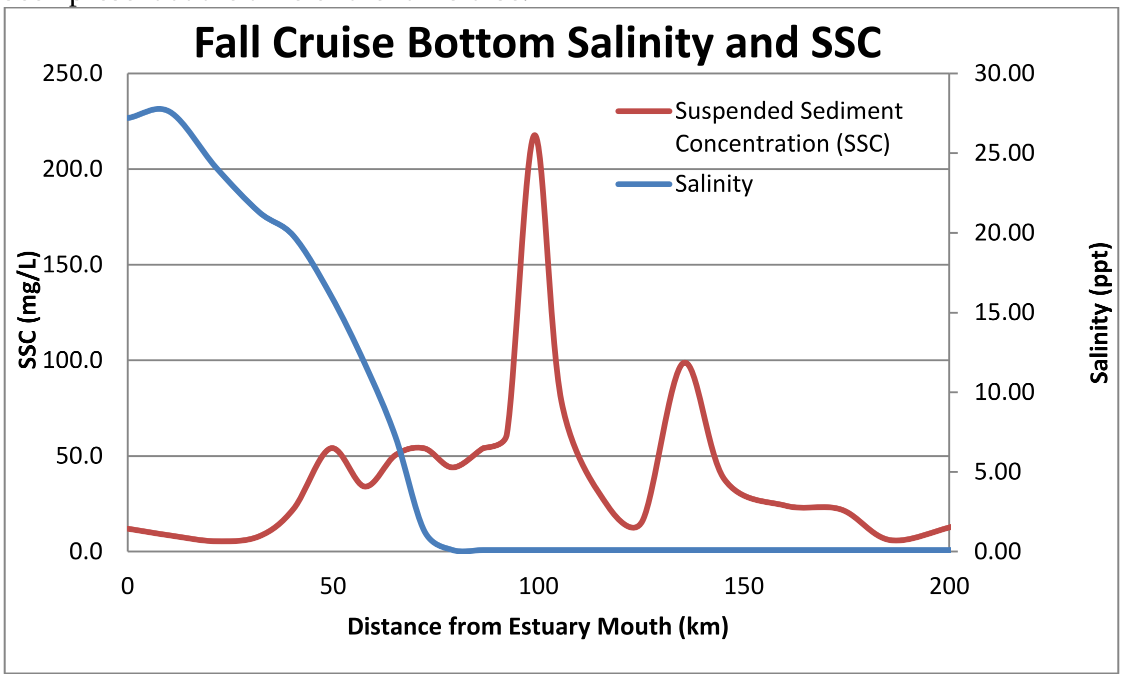

Figure 14 Bottom Suspended Sediment Concentration and Salinity from an axial survey of the estuary during the fall cruise.

Cores from the fall cruise show a notable change in depositional patterns when compared to the summer cores. Primarily, it appears that the main depocenter has shifted from the middle estuary to the lower estuary. At the time of the cruise, the ETM was seen at about 100 km landward of the bay mouth. However, the large amounts of deposition at site I suggests the ETM had shifted up to 50 km seaward during the storm events allowing large amounts of deposition to occur in the lower estuary. Nichols (1993) saw a similar reaction to a storm event in the Chesapeake

Estuary as a result of high fresh water discharge. In addition to high activity levels of Be-7 at site I, I-131 was present in the top 6 cm. Since radioiodine is only introduced to the water column in the urbanized estuary which ends at Wilmington, DE, I-131 tagged sediment must have been transported at least 50 km to be deposited at site I. It is unclear if the source of the tagged sediment was from the water column or resuspended bed sediment from near site A. However, low Be-7 activity and no I-131 activity at site A indicate that the area was likely scoured during the high discharge period.

Winter

Cores from the winter cruise were essential to understanding how the estuary recovered following the large storm events in the fall. The time between the fall and winter cruises should have allowed the system to return to a more normal state. There were, however, multiple periods of high freshwater discharge prior to the winter cruise which may have again disrupted the sediment system. Figure 15 shows that SSC varied greatly and that a single ETM was not easily distinguishable.

There are two major changes between the fall and winter cores. First, site A again showed significant deposition in winter; there was little no none in fall. Second, site I no longer showed high rates of deposition in the winter. Also, no radioiodine was present at I in the winter. These changes suggest that by the time of the winter cruise, the ETM and primary depocenter had migrated back to the area of site A. It cannot, however, be determined if any sediment deposited at site I during the fall was transported back to site A in the gravitational circulation.

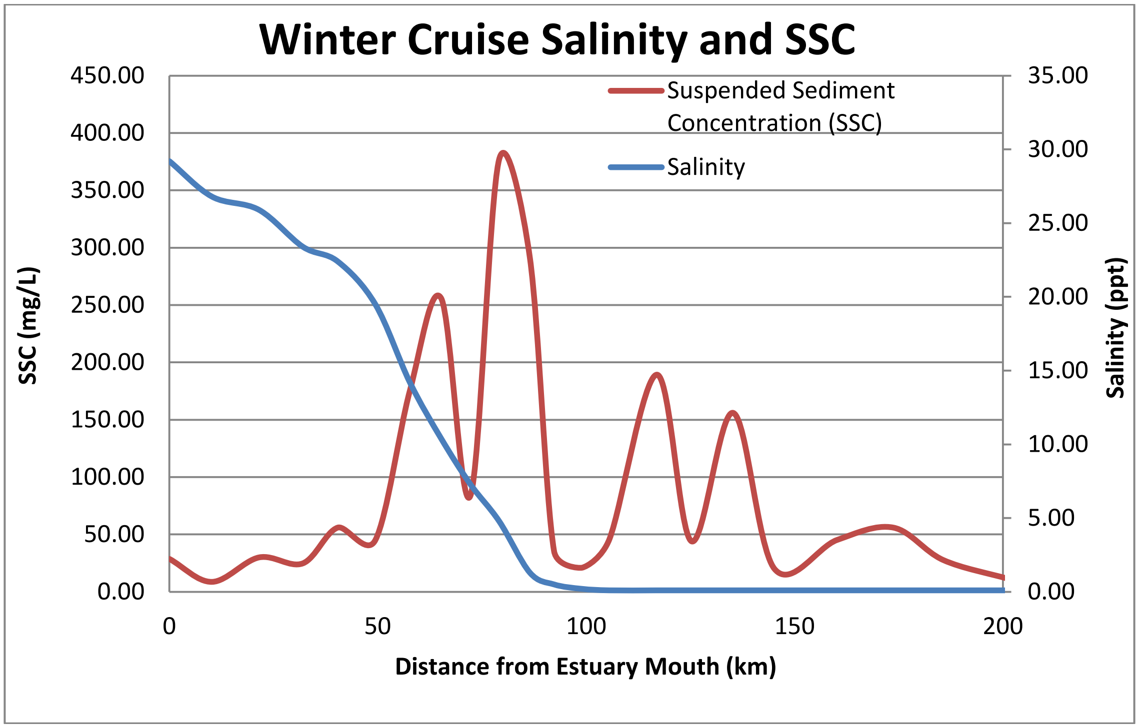

Figure 15 Bottom Suspended Sediment Concentration and Salinity from an axial survey of the estuary during the winter cruise.

Seasonal Variations

During the summer, the greatest deposition rate was found at site A, though site I actually showed the highest inventory of Be-7. Given the dry bulk density for the core taken at site I in the summer (Figure 5-a), sand may have been present near the surface and distorted the Be-7 activity measurements taken. In fall, the greatest deposition was clearly seen at site I. Radioiodine was measured in the top 6 cm of core suggesting sediment from the middle estuary was being transported to the lower estuary before being deposited. Based on the predictions made by Nichols (1993) on coastal plain estuary's response to storm events, it is probable that high levels of freshwater input pushed the ETM up to 50 km seaward. This is evinced by extremely high depositional patterns at site I and lowered depositional patterns at site A. Information from the winter cruise suggests the estuary's sediment dynamics had at least partially returned to a normal state. In winter, significant deposition was found at Site A as determined by Be-7and I-131 activity. Deposition was much lower at site I and no radioiodine were measured.

To estimate the depositional patterns at each site from season to season, the Residual Inventory Method was used as described by Canuel et al (1990). By decay correcting the Be-7 activity at a site from the prior season, an expected inventory was calculated for fall and winter. The expected inventory represents the inventory resulting from decay of the radionuclides between sampling dates only. The decay corrected value was then compared to the measured value at each site.

Site A showed a decreasing inventory with each consecutive measurement (Figure 16). However, the measured inventory was higher than the expected inventory in fall and winter suggesting at least some deposition likely occurred during the intervening time. It does appear that there was little deposition from fall to winter. The sediment system landward of site A may have been partially scoured during multiple storm systems during the fall and winter, lowering the source of new sediment to the recovering system.

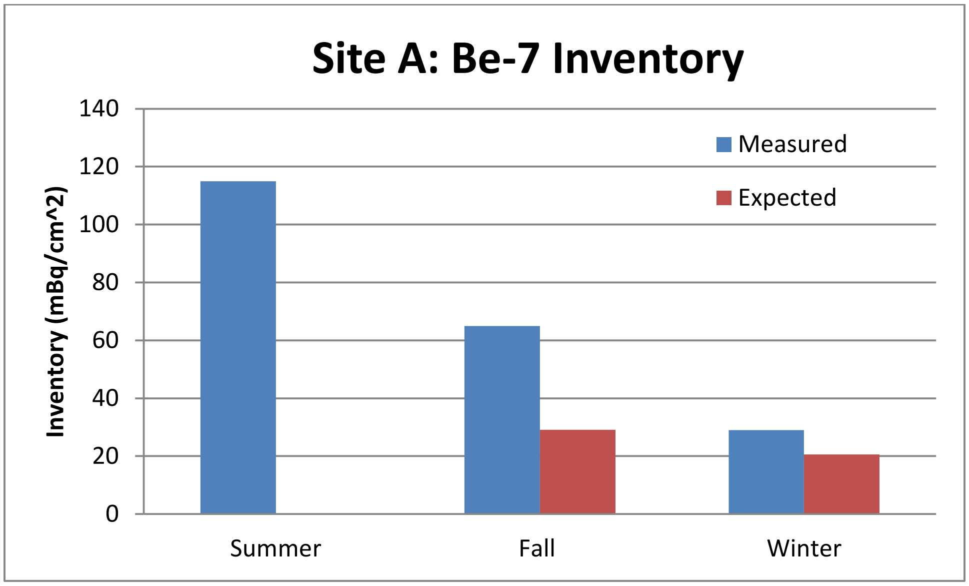

Figure 16 Measured and expected Be-7 inventories at site A for each season

Figure 17 shows the measured and expected inventories for site F. The most notable deviation occurs during the fall when the measured inventory is over 50 mBq/cm^2 higher than the expected inventory. This large increase in inventory is believed to be a result of the fall storms which pushed the ETM seaward and increased deposition in the area of sites F and I. The measured inventory for site I was about 100 mBq/cm^2 higher than the expected value in fall (Figure 18), further evidence that deposition was high in this area prior to measurement. Another important factor regarding seasonal variations in deposition are the winter inventory values for sites F and I (Figure18). Both sites showed a measured value near the expected value, an indicator that there was little deposition in that area of the lower estuary from fall to winter, a significant change from the summer to fall time period.

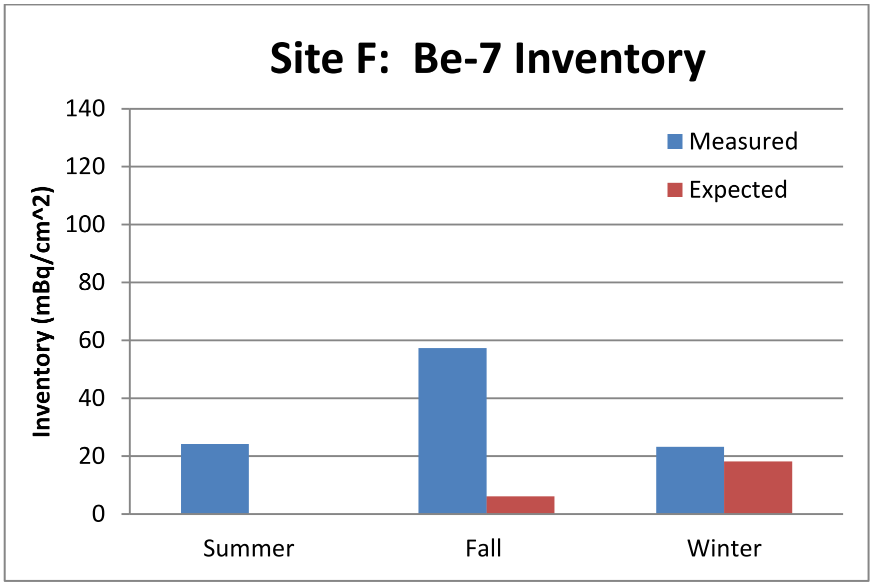

Figure 17 Measured and expected Be-7 inventories at site F for each season

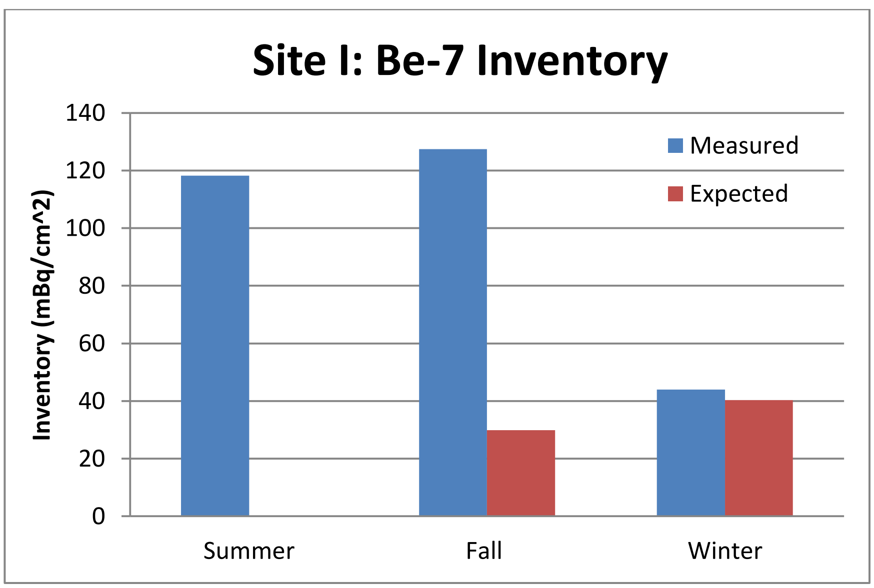

Figure 18 Measured and expected Be-7 inventories at site I for each season

Chapter 5

SUMMARY AND CONCLUSIONS

This study used radionuclides that absorb to fine grain sediment to analyze seasonal depositional patterns in the Delaware Estuary. The project also studied the effects of an episodic storm event on the estuary's sediment dynamics. Using depositional information derived from radionuclide analysis, it was determined that there were significant changes in deposition rates and deposition location between seasons.

Summer was the first measured season in the project and it followed a time of relatively normal fresh water discharge. Therefore, it was used as a base model to compare other seasons to. Fall, by comparison, had dramatically different depositional patterns than summer. Primarily, the depocenter seemed to shift from the middle estuary in the vicinity of site A down to the lower estuary in the area of sites F and I. In winter, it appeared that the sediment system was beginning to return to a normal state, but that deposition was generally less at all sites. This could be the result of a of the sediment source being flushed by large fresh water discharges in fall and winter. Predictions made from measurements in this project are in accordance with other estuarine studies (Sommerfield, 2007, Nichols, 1993). Still, further work must be done to better understand the Delaware Estuary's sediment system and radionuclides as measuring tool for sediment deposition.

To date, relatively little work has been done on the use of I-131 as a sediment tracer, but Sommerfield is continuing his studies on the use of radioiodine as a source specific sediment tracer. In general, further studies on sediment deposition will help to clarify more specific areas of deposition in the Delaware Estuary. Cores near the sides of the estuary and in the mud flats would help to determine where any resuspended sediment is ultimately being deposited. Finally, while this study revealed valuable information regarding bottom sediment dynamics, the results could be interpreted better with a more encompassing understanding of the Delaware Estuary's sediment system. Studies currently being conducted by Sommerfield and Duval on the water column's sediment dynamics will help to relate suspended sediment concentrations and hydrodynamics to bottom deposition.

REFERENCES

1. Blanton, J.O., Amft, J., Tisue, T., 1997. Response of a Small-Scale Bottom-Attached Estuarine Plume to Wind and Tidal Dissipation. *Journal of Coastal Research*. **13**. 2. 349-362

2. Biggs, R.B., Sharp, J.H., Church, T.M. and Tramontano, J.M., 1983. Optical properties, suspended sediments, and chemistry associated with the turbidity maxima of the Delaware Estuary. Can. J. Fish. Aquat. Sci. 40 (Suppl. 1): 172-179

3. Biggs, R.B., and Beasley, E.L., 1988. Bottom and suspended sediments in the Delaware River and estuary. *Ecology and Restoration of the Delaware River basin. Majumdar*, S.K., Miller, E.W., Sage, L.E. 116-130

4. Bolin, B. and Rodhe, H. 1973. A note on the concepts of age distribution and transit time in natural reservoirs. Tellus, 25: 58–62.

5. Botton, M.L., and Loveland, R.E., 2003. Abundance and Dispersal Potential of horseshoe Crap (Limulus polyphemus) Larvae in the Delaware Estuary. *Estuaries*, **26**, 6, 1472-1479.

6. Canuel, E.A., Martens, C.S., Benninger, L.K., 1990. Seasonal variations in Be-7 activity in the sediments of Cape Lookout Bight, North Carolina. Geochimical et CosmochimicaActa 54, 237Ğ245.

7. Cook T.L., Sommerfield C.K., Wong K-C., 2002. Observations of tidal and springtime sediment transport in the upper Delaware Estuary*. Estuarine, Coastal and Shelf Science*, **72**, 1-2, 235-246.

8. Fitzgerald, S.A., Klump J.V., Swarzenski, P.W., Mackenzie, R.A., Richards, K.D., 2001. Beryllium-7 as a tracer of short-term sediment deposition and resuspension in the Fox River, Wisconsin. *Environmental Science and Technology* **35**(2): 300-305.

9. Garvine, R.W., McCarthy, R.K., Wong, K.-C., 1992. The axial salinity distribution in the Delaware Estuary and its weak response to river discharge. *Estuarine, Coastal and Shelf Science.***35**, 157-165

10. Gibbs, R., Suspended sediment transport and the turbidity maximum, in Estuaries, geophysics and the environments and facies, C. Officer, p. 104-109, National Academy of Sciences, Wash. D.C., 1977.

11. Howel, A., 2011. Delaware Estuary. *Mid-Atlantic Water*. June 21, 2011.

12. Matisoff, G., Wilson, C.G., Whiting, P.J., 2005. The $^{7}Be/^{210}Pb_{xs}$ ratio as an indicator of suspended sediment age or fraction new sediment in suspension. *Earth Surf. Process. Landform***30**, 1191-1201.

13. Meade, R.H., 1969. Landward transport of bottom sediments in estuaries of the Atlantic coastal plain*. Journal of Sedimentary petrology*. **39**. 1. 222-234.

14. Meade, R.H., 1982. Sources, sinks, and storage of river sediment in the atlantic drainage of the united states. *The Journal of Geology*. **90**, 3, 235-251.

15. Nichols, M.M., and Biggs, R.B., 1985. Estuaries. *Coastal Sedimentary Environments*, Davis R.A. 715.

16. Nichols, M. M., 1993. Response of Coastal Plain Estuaries to Episodic Events in the Chesapeake Bay Region. *Nearshore and Estuarine Cohesive Sediment Transport – Coastal and Estuarine Studies*, **42**, 1-20

17. Olsen, C.R., Larsen, I.L., Lowry, P.D., and Cutshall, N.H. 1986. Geochemistry and Deposition of ^{7}Be in River-Estuarine and Coastal Waters. *Journal of Geophysical Research*, **91**, C1, 896-908.

18. Sharp, J.H., Cifuentes, L.A., Coffin, R.B., Pennock, J.R., and Wong, K-C., 1986. The influence of river variability on the circulation, chemistry, and microbiology of the Delaware estuary. *Estuaries*. **9**, 4A, 261-269.

19. Smith J.P., Oktay S.D., Kada J., Olsen C.R. 2008. Iodine-131: A potential Short-Lived Wastewater-Specific Particle Tracer in an Urbanized Estuarine System. *Environmental Science Technology***42**: 5435-5440.

20. Sommerfield C.K., and K.-C Wong. 2011. Mechanisms of sediment flux and turbidity maintenance in the Delaware Estuary. *Journal of Geophysical Research*. **116**, C01005, 16.

21. Sommerfield, C.K. and Duval, D., 2012. Radioiodine (I-131) as a tracer of estuarine transport processes. Eos Transactions, American Geophysical Union, Ocean Sci. Meet. Suppl., Abstract 10339.

22. U.S. Geological Survey. 2011. Water Resources Data for New Jersey. Water Year 2011. Delaware River Basin and Tributaries to the Delware Bay. U.S. Geological Survey Water Data Report NJ.

23. WallBrink, P.J., Walling, D.E., He, Q., 2002. Radionuclide Measurement using HPGe Gamma Spectrometry. *Handbook for the assessment of soil erosion and sedimentation using environmental radionuclides*. 67-96.

24. Weil, C,B., 1977. Sediments, structural framework, and evolution of Delaware Bay, A transgresssive estuarine delta.*Sea Grant Technical Report No. DEL-SG-4-77*. 199.

25. Woodruff, J.D., Geyer, W.R., Sommerfield, C.K., and Driscoll, N.W., 2001. Seasonal variation of sediment deposition in the Hudson River estuary. *Marine Geology*.**179**. 105-119.

Appendix A

SUMMER RADIONUCLIDE AND DENSITY DATA

Core	Interval (cm)	Be-7 Specific Activity (mBq/g)	I-131 Specific Activity (mBq/g)	Pb-210$_{xs}$ Specific Activity (mBq/g)	Dry Bulk Density (g/cm^3)
36	0-2	25.49 ± 1.97	49.03 ± 1.82	59.39 ± 5.16	0.44
36	2-4	21.45 ± 1.57	28.12 ± 1.38	53.06 ± 4.26	0.42
36	4-6	15.76 ± 1.31	8.16 ± 1.05	66.79 ± 4.40	0.43
36	6-8	10.34 ± 1.27	-0.86 ± 1.03	66.87 ± 4.15	0.48
36	8-10	11.24 ± 1.21	-1.61 ± 0.97	92.26 ± 4.37	0.44
36	10-12	8.46 ± 1.36	1.99 ± 1.00	94.12 ± 4.72	0.41
36	12-14	6.99 ± 1.18	0.69 ± 0.94	82.01 ± 4.25	0.47
36	14-16	7.60 ± 1.07	0.49 ± 0.95	73.75 ± 3.95	0.47
36	16-18	8.57 ± 1.13	1.99 ± 0.97	83.53 ± 4.39	0.42
36	18-20	4.82 ± 1.20	0.73 ± 0.98	84.23 ± 4.40	0.54
36	20-22	4.45 ± 0.95	-2.69 ± 0.94	74.24 ± 3.95	0.53
36	22-24	4.24 ± 1.05	1.21 ± 0.93	81.09 ± 4.30	0.45
36	24-26	4.48 ± 2.61	1.04 ± 2.20	116.49 ± 8.94	0.09
37	0-2	10.01 ± 0.89	12.73 ± 0.80	13.59 ± 3.46	0.78
37	2-4	0.44 ± 0.39	0.92 ± 0.35	9.99 ± 2.73	0.92
38	0-2	0.30 ± 0.46	1.85 ± 0.48	71.46 ± 4.68	0.50
		±	±	±	
39	0-2	0.86 ± 0.49	1.07 ± 0.51	2.84 ± 3.23	0.78
40	0-2	-0.83 ± 0.51	0.55 ± 0.46	61.88 ± 4.86	0.50
41	0-2	4.02 ± 0.65	-0.34 ± 0.33	11.90 ± 2.70	0.80
41	2-4	4.42 ± 0.60	-0.29 ± 0.35	15.88 ± 2.71	1.07
41	4-6	3.55 ± 0.56	-0.46 ± 0.34	24.34 ± 2.94	0.90
41	6-8	1.18 ± 0.40	0.34 ± 0.35	18.94 ± 3.15	1.03
41	8-10	-0.25 ± 0.39	-1.53 ± 0.41	35.04 ± 3.48	0.74
41	10-12	0.47 ± 0.36	3.38 ± 0.36	19.26 ± 2.90	0.85
41	12-14	0.26 ± 0.31	-0.11 ± 0.33	7.39 ± 2.73	1.10
41	14-16	-0.09 ± 0.27	0.93 ± 0.31	1.85 ± 2.20	1.10
41	16-18	0.96 ± 0.33	0.64 ± 0.37	5.93 ± 2.47	0.94
41	18-20	-0.32 ± 0.36	0.54 ± 0.37	0.86 ± 2.15	0.90
41	20-22	0.67 ± 0.32	-0.09 ± 0.36	3.16 ± 2.29	1.03
42	0-2	0.61 ± 0.25	-0.15 ± 0.21	1.10 ± 1.28	1.59
43	0-2	1.99 ± 0.89	2.75 ± 0.82	30.08 ± 3.21	0.67
44	0-2	9.80 ± 0.94	-0.44 ± 0.43	37.73 ± 3.51	0.67
44	2-4	13.39 ± 1.00	0.89 ± 0.41	52.25 ± 3.65	0.64
44	4-6	14.32 ± 0.98	0.07 ± 0.38	45.41 ± 3.94	0.66
44	6-8	25.70 ± 1.27	0.25 ± 0.47	86.11 ± 4.74	0.41
44	8-10	23.64 ± 1.28	-0.59 ± 0.50	100.94 ± 4.55	0.41
44	10-12	15.04 ± 1.02	-0.95 ± 0.46	77.53 ± 4.35	0.52
44	12-14	10.17 ± 0.89	0.51 ± 0.43	53.88 ± 3.98	0.64
44	14-16	1.62 ± 0.56	-0.85 ± 0.46	43.68 ± 4.13	0.54
44	16-18	0.05 ± 0.41	1.02 ± 0.40	13.49 ± 3.61	0.63
44	18-20	-0.26 ± 0.40	-0.11 ± 0.43	-0.46 ± 2.62	0.80

Appendix B

FALL RADIONUCLIDE AND DENSITY DATA

Core	Interval (cm)	Be-7 Specific Activity (mBq/g)			I-131 Specific Activity (mBq/g)			$Pb\text{-}210_{xs}$ Specific Activity (mBq/g)			Dry Bulk Density (g/cm^3)
45	0-2	13.04	±	1.80	1.97	±	1.11	74.747	±	12.6	0.39
45	2-4	12.31	±	1.07	1.68	±	0.57	39.532	±	3.97	0.47
45	4-6	7.02	±	1.26	-0.11	±	0.59	79.084	±	4.74	0.35
45	6-8	10.00	±	0.99	0.39	±	0.50	52.243	±	3.95	0.44
45	8-10	8.04	±	1.05	-0.26	±	0.54	72.152	±	4.4	0.44
45	10-12	8.80	±	1.04	-0.52	±	0.58	61.3	±	4.09	0.43
45	12-14	2.85	±	0.66	0.64	±	0.46	31.821	±	3.52	0.65
45	14-16	2.32	±	0.69	-0.45	±	0.48	36.639	±	3.47	0.66
45	16-18	1.94	±	0.56	0.71	±	0.43	34.019	±	3.45	0.69
45	18-20	2.32	±	0.64	0.08	±	0.45	40.869	±	4.05	0.65
45	20-22	1.54	±	0.51	-0.44	±	0.39	35.702	±	3.51	0.85
45	22-24	0.84	±	0.47	-0.52	±	0.44	34.517	±	3.2	0.73
45	24-25	0.04	±	0.49	-0.53	±	0.47	81.488	±	3.9	0.57
47	0-2	8.12	±	1.07	0.88	±	0.93	43.194	±	2.9	0.52
48	0-2	-0.24	±	0.48	1.22	±	0.49	12.82	±	3.15	0.61
49	0-2	6.021	±	0.62	-1.53	±	0.29	9.458	±	1.85	1.05
49	2-4	7.593	±	0.75	1.19	±	0.58	5.398	±	1.85	1.04
49	4-6	13.545	±	0.82	0.86	±	0.57	25.216	±	2.14	0.71
49	6-8	3.855	±	0.61	-0.35	±	0.32	20.683	±	2.22	0.82
49	8-10	1.98	±	0.46	0.05	±	0.33	20.995	±	2.44	0.84
49	10-12	1.03	±	0.48	0.06	±	0.59	15.956	±	1.94	1.00
49	12-14	0.16	±	0.27	-0.16	±	0.26	18.235	±	1.99	0.91
49	14-16	-0.51	±	0.32	-2.63	±	0.30	23.406	±	2.21	0.76
49	16-18	-0.21	±	0.29	-0.19	±	0.32	15.793	±	1.77	1.02
49	18-20	-0.62	±	0.32	-0.07	±	0.32	17.922	±	1.93	0.97
49	20-22	0.03	±	0.23	-0.03	±	0.25	6.552	±	1.68	1.28
51	0-2	-0.36	±	0.62	-0.50	±	0.53	40.71	±	3.68	0.47
51	2-4	0.3	±	0.39	0.32	±	0.45	30.178	±	3.48	0.58
51	4-6	-0.59	±	0.38	0.05	±	0.39	22.828	±	2.82	0.84
52	0-2	56.869	±	2.09	25.31	±	1.19	100.199	±	4.3	0.28
52	2-4	33.613	±	1.4	16.94	±	0.83	56.262	±	3.09	0.41
52	4-6	33.29	±	1.44	9.44	±	0.80	60.992	±	3.44	0.43
52	6-8	31.435	±	1.36	0.88	±	0.52	55.999	±	3.25	0.43
52	8-10	8.184	±	0.72	-0.24	±	0.33	35.426	±	2.4	0.64
52	10-12	2.115	±	0.57	-0.83	±	0.46	46.102	±	3.29	0.64
52	12-14	0.36	±	0.39	-0.05	±	0.33	10.378	±	1.99	0.78
52	14-16	0.58	±	0.44	0.50	±	0.42	5.675	±	2.21	0.67
52	16-18	0.29	±	0.37	0.39	±	0.41	-1.958	±	2.13	0.77
52	18-20	0.27	±	0.34	-0.45	±	0.28	6.894	±	2.01	0.89
52	20-22	0.34	±	2.05	-0.16	±	0.32	19.282	±	1.86	0.76

Appendix C

WINTER RADIONUCLIDE AND DENSITY DATA

Core	Interval (cm)	Be-7 Specific Activity (mBq/g)			I-131 Specific Activity (mBq/g)			$Pb\text{-}210_{xs}$ Specific Activity (mBq/g)			Dry Bulk Density (g/cm^3)
53	0-2	10.63	±	0.96	8.24	±	0.72	31.652	±	3.86	0.61
53	2-4	14.29	±	1.03	9.85	±	0.75	27.766	±	2.74	0.41
53	4-6	2.97	±	0.72	0.84	±	0.56	69.821	±	4.38	0.37
53	6-8	2.46	±	0.83	-0.44	±	0.62	85.069	±	4.67	0.35
54	0-2	10.58	±	0.80	3.43	±	0.73	10.7	±	2.07	0.73
54	2-4	12.72	±	0.95	0.43	±	0.51	27.552	±	2.77	0.65
54	4-6	14.07	±	0.99	0.55	±	0.85	23.474	±	2.84	0.70
54	6-8	14.07	±	1.04	0.50	±	0.81	28.776	±	2.65	0.69
54	8-10	10.09	±	0.95	-0.35	±	0.77	18.174	±	2.41	0.86
54	10-12	8.16	±	0.93	0.71	±	0.78	25.716	±	2.63	0.86
54	12-14	9.42	±	1.11	-2.51	±	0.97	38.67	±	3.35	0.71
55	0-2	-0.887	±	0.53	-0.68	±	0.57	64.2	±	4.26	0.54
56	0-2	-0.209	±	0.58	0.83	±	0.58	30.124	±	3.56	0.61
57	0-2	14.199	±	1.03	1.49	±	0.51	59.127	±	4.19	0.49
57	2-4	4.235	±	0.71	-0.40	±	0.43	40.417	±	3.19	0.57
57	4-6	5.211	±	0.77	-0.38	±	0.43	46.741	±	3.74	0.44
57	6-8	0.604	±	0.45	0.25	±	0.33	21.23	±	2.61	0.77
57	8-10	0.461	±	0.31	-0.29	±	0.29	10.196	±	2.04	1.04
57	10-12	0.405	±	0.35	-0.66	±	0.33	15.466	±	2.23	0.89
57	12-14	0.161	±	0.34	-0.22	±	0.35	22.125	±	2.88	0.97
57	14-16	0.683	±	0.35	-0.19	±	0.35	26.419	±	2.72	0.81
59	0-2	-0.306	±	0.56	-0.26	±	0.51	17.477	±	2.6	0.72
60	0-2	15.211	±	1.11	-0.31	±	0.53	46.843	±	3.17	0.47
60	2-4	16.233	±	1.09	-1.64	±	0.62	62.998	±	3.21	0.41
60	4-6	4.365	±	0.72	-1.11	±	0.57	32.083	±	2.84	0.58
60	6-8	7.322	±	0.8	0.11	±	0.48	38.24	±	2.74	0.54
60	8-10	2.278	±	0.51	0.61	±	0.40	29.921	±	3.5	0.71
60	10-12	0.701	±	0.37	0.187	±	0.33	22.069	±	2.84	0.93